Dynamics Reconstruction of Remote Photoplethysmography

Lin He(✉), Kazi Shafiul Alam, Jiachen Ma, Richard Povinelli, and Sheikh Iqbal Ahamed

Marquette University, Milwaukee, WI, USA
lin.he@marquette.edu

Abstract. Photoplethysmography based medical devices are widely used for cardiovascular status monitoring. In recent years, many algorithms have been developed to achieve cardiovascular monitoring results comparable to the medical device from remote photoplethysmography (rPPG). rPPG is usually collected from the region of interest of the subject face and has been used for heart rate detection. Though there were many works on the study of chaos dynamics of PPG, very few are on the characteristics of the rPPG signal. The main purpose of this study is to discover rPPG dynamics from nonlinear signal processing techniques, which may provide insight for improving the accuracy of cardiovascular status monitoring. Univ. Bourgogne Franche-Comté Remote PhotoPlethysmoGraphy dataset is used for the experiment. The results show rPPG is considered as chaotic. The best-estimated embedding dimension for the rPPG signal is between 3 to 4. The time delay is 10 for an interpolated 240 Hz rPPG signal. The interpolation process will increase the complexity level and reduce the correlation dimension of the rPPG. The bandpass filtering process will reduce the complexity level and the correlation dimension of the rPPG. Introducing the features derived from reconstructed phase space such as Lyanpunov exponent, correlation dimension and approximate entropy, could improve the accuracy of heart rate variability detection from rPPG.

Keywords: Remote photoplethysmography · Phase space reconstruction · Heart rate · Heart rate variability

1 Introduction

Cardiovascular disease is one of the most prevalent diseases for adults over 20 years old in the United States [1]. Photoplethysmography (PPG) based medical devices are widely used for cardiovascular health monitoring in clinical settings. PPG is a typical noninvasive method that measures subtle changes in the light reflection from human skin due to the blood volume variations through the cardiovascular pulse cycle [2]. Professional PPG measurement devices are expensive

H. Lewy and R. Barkan (Eds.): PH 2021, LNICST 431, pp. 96–110, 2022.
https://doi.org/10.1007/978-3-030-99194-4_8

and uncomfortable to use. In recent years, several algorithms have been developed to achieve heart rate (HR) and heart rate variability (HRV) results similar to professional devices through remote PPG (rPPG), which uses a camera to collect a video of the region of the skin from a distance instead of using near-infrared light for PPG recording. The rPPG signals could be extracted from the video recordings and provide similar health monitoring results to PPG signals.

There are many works about nonlinear analysis of the PPG signals to improve the detection accuracy and discover underlying characteristics of the PPG signals. PPG signals collected from healthy young human subjects is consistent with the definition of chaos movement [3]. The method of phase space reconstruction has been applied to PPG signals and shows PPG can provide an earlier warning of deterioration based on PPG signals because it provides a similar trend for the parameters derived from arterial blood pressure (ABP) [4]. There are also studies on PPG signals collected not from near-infrared light. The experiment results show the PPGs collected under the red or green light is chaotic [5].

In addition to PPG, nonlinear signal processing techniques also apply to the rPPG. It is possible to use phase space reconstruction on the rPPG signals collected from the skin of the wrist. The interpolated and filtered signals can be considered as noise-contaminated deterministic signals [6]. However, the previous studies are based on PPG signals with a high sampling rate, mostly 200 Hz or the study of the rPPG collected in an area with little noise and motion. There has been little work on rPPG chaotic analysis based on video collected from the face, which has a lower sampling rate 30 Hz and large noise due to the distance and the motion of the body. In this paper, we present the analysis of the chaotic dynamics of rPPG collected from human face videos.

The contribution of this paper is as follows:

- We compared the chaotic dynamics for different PPG and rPPG signals.
- We use the phase space reconstruction method to discover the underlying characteristics of rPPG.
- We showed introducing the features derived from reconstructed phase space could improve the accuracy of HRV detection.

The structure of the remaining parts of the paper is as follows: In Sect. 2, we present the method we used for rPPG extraction. Section 3 evaluates the results of the dynamics of PPG and rPPG signals. In Sect. 4, we present conclusions.

2 Related Works

2.1 rPPG Extraction Methods

PPG signals can be collected from fingertips positioned on a smartphone camera [7]. However, this method still requires the subject to stay in a fixed position, which has the same disadvantage of traditional methods. Poh et al. [8] proposed a new non-contact method, which is known as remote PPG (rPPG). The method uses the front face of the phone camera to extract PPG signals

and heart rate measurements has a $RMSE < 5bpm$ and a correlation of 0.95. [9] extends the work by using CHROM for rPPG extraction for heart rate detection. This method is further implemented by [10], which provides an algorithm with improvement in the detection accuracy for heart rate and heart rate variability for low-resolution videos. [11] proved the Plane orthogonal to the Skin-tone method (POS) can generate a better quality signal than CHROM for heart rate measurement. It also compared the signal to noise ratio (SNR) of different rPPG extraction approaches and proved the rPPG from POS has an average SNR of 5.16, which is larger than all the other approaches. Table 1 shows the different related works on rPPG extraction algorithm developed over the years.

Table 1. Algorithms on rPPG extraction

Ref.	ROI	Algorithm	Parameter	Year
Poh et al. [8]	Face	BSS	HR	2010
Lewandowska et al. [12]	Forehead	ICA	HR	2012
de Haan et al. [9]	Face	CHROM	HR	2013
de Haan et al. [13]	Face	PBV	HR	2014
Wang et al. [14]	Face	2SR	HR	2016
Huang et al. [10]	Face	CHROM	HR, HRV	2016
Wang et al. [11]	Face	POS	HR	2017

2.2 Dataset Used for rPPG Testing

Many efforts have been made in recent years on studying the rPPG algorithms on heart rate with existing public datasets such as MAHNOB and MMSE-HR. However, these videos are under strong compression making valuable information impossible to extract [15]. Normally heart rate estimation requires a lower quality video than heart rate variability. An uncompressed video data set is required to derive the best results of heart rate variability. We developed the algorithms and compared the performance on the public data set UBFC-rPPG.

Univ. Bourgogne Franche-Comte Remote PhotoPlethysmoGraphy (UBFC-rPPG) is a data set proposed for remote PPG (rPPG) studies [16]. Subject faces were recorded using a webcam (Logitech C920 HD Pro) at 30fps and a resolution of 640 × 480. The video file is an avi file in an uncompressed 8-bit RGB format. The ground truth PPG signal wave was recorded using the CMS50E transmissive pulse oximeter. It is a popular data set used for the validation of different rPPG approaches. The video files and ground truth data are used in this research.

3 rPPG Extraction Method

Our approach mainly follows the method proposed by Huang et al. [10]. Some recent enhancements such as amplitude selective filtering [20] and plane orthogonal to skin tone method [11] are included. The flowchart of the whole method is in Fig. 1.

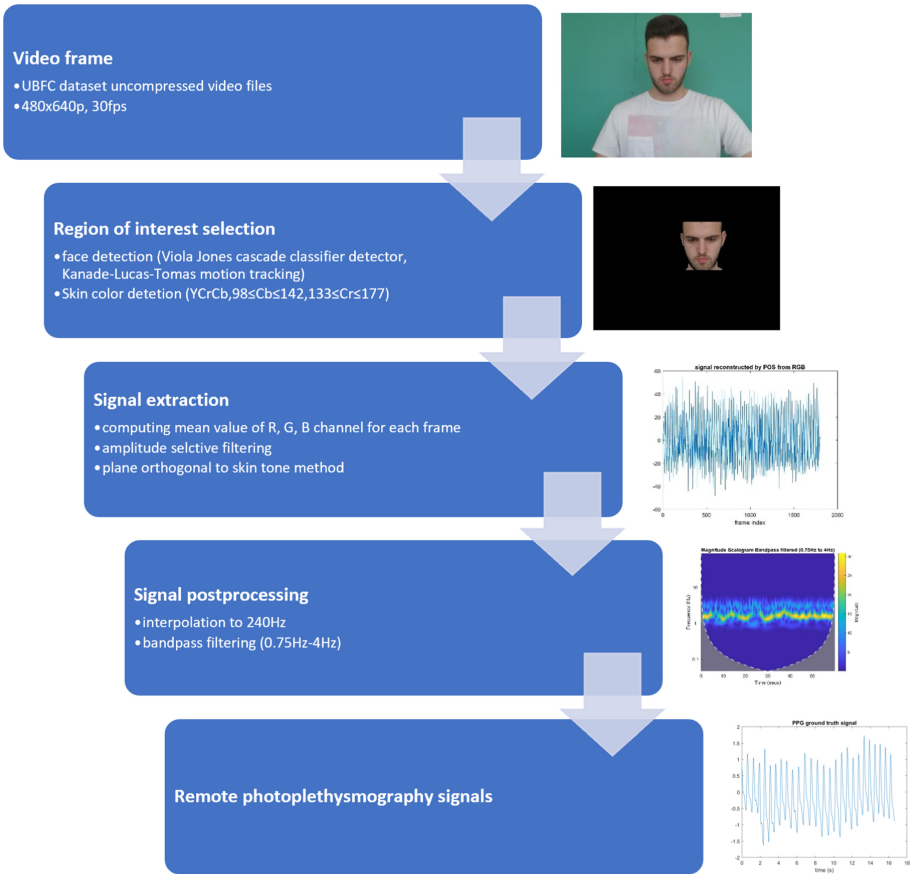

Fig. 1. Method overview

3.1 Region of Interest Selection

The region of interest (ROI) is first selected by the face detection algorithm using Viola-Jones detection [17] and Kanade-Lucas-Tomasi [18] for motion tracking. After the face detection algorithm locates the position of the face in a rectangular bounding box, the skin detection algorithm is applied to the ROI to select the skin pixels in the YCrCb color space [19]. As provided, a pixel is detected as skin if $98 \leq Cb \leq 142, 133 \leq Cr \leq 177$.

3.2 Signal Extraction

After the skin pixels are selected from the ROI, the mean value of the RGB channels of each frame is calculated to form a series of raw signals of R, G, B channel. Then, amplitude selective filtering [20] is used to eliminate noise distortions from the signals. The plane orthogonal to the Skin-tone method [11] is used to extract pulse signals from the RGB signals. It assumes the RGB signals are the mixture result from three different source signals. One of them is the pulse signal and the others are light sources or background noise. The algorithm is based on the study of the optical and physiological model of the skin reflection and can separate the pulse signal that is independent of the skin tone and the light source. The result from [11] shows rPPG from POS has an average SNR of 5.16, which is larger than all the other extraction methods.

3.3 Signal Postprocessing

After the pulse signal is extracted, postprocessing steps are used for denoising. Because the signal is sampled 30 Hz, interpolation 240 Hz is needed to smooth the signal.

There are many approaches for post-processing the rPPG signal. The most widely used approach is bandpass filtering, which is to select only the magnitude of the signal within the pulse rate range (0.75 Hz 4 Hz) and to use inverse wavelet transformation to reconstitute the signal.

4 Chaotic Dynamics Analysis of PPG and rPPG

4.1 PPG and rPPG Signals

UBFC-rPPG is a dataset containing video data of an average length of 1 min. Logitech C920 HD Pro is used to collect the video of the frontal face at a distance of about 1 m from the camera. All experiments are conducted indoors with varying amounts of sunlight and indoor illumination. The recordings have an uncompressed AVI format at 30 fps and a resolution of 640 × 480. The ground truth PPG signal was recorded simultaneously using the CMS50E transmissive pulse oximeter. An example of the ground truth PPG signal is in Fig. 2.

Based on the data provided by the UBFC-rPPG data set, we extract 4 signals for phase space reconstruction. The ground truth PPG signal is not uniformly sampled. To apply the approach, we interpolate the ground-truth signal 240 Hz by linear spline (PPG 240 Hz). The rPPG signal is extracted from the video files at an original frequency 30 Hz (rPPG 30 Hz) and interpolated 240 Hz (rPPG 240 Hz). Then the signal is bandpass filtered by the continuous wavelet transformation (rPPG filtered).

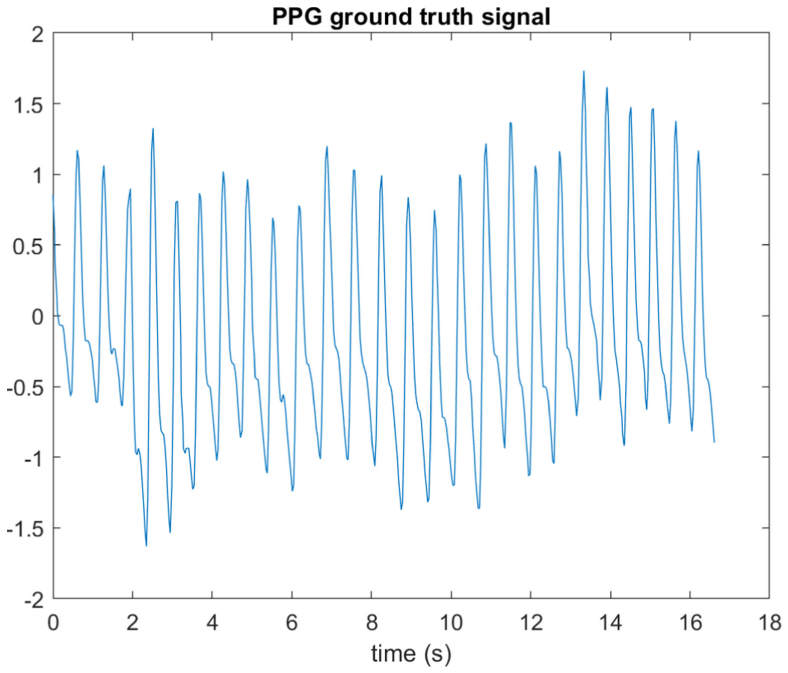

Fig. 2. Ground truth PPG signal

4.2 Phase Space Reconstruction

A uniformly sampled time series signal with a single variable $X = (x_1, x_2, x_3 \ldots x_n)$ can be reconstructed a phase space which has m-dimension. If the embedding method uses time lag τ, the delayed reconstruction has coordinates as $X_r = (x_j, x_{j+\tau}, \ldots x_{j+(m-1)\tau})$.

The time delay τ can be estimated by finding the first minimum value of the average mutual information (AMI), which is computed as

$$AMI(t) = \sum_{i=1}^{N} p(x_i, x_{i+t}) log_2[\frac{p(xi, x_{i+t})}{p(x_i)p(x_{i+t})}] \tag{1}$$

where N is the length of the signal and t is the time lag.

The embedding dimension m can be estimated using the false nearest neighbor algorithm. For a dimension m, the points X_i^r and nearest point X_i^{r*} are false neighbors if

$$\sqrt{\frac{D^2(m+1) - D^2(m)}{D^2(m)}} > Threshold \tag{2}$$

where $D^2(m) = ||X_i^r - X_i^{r*}||^2$.

The result for the estimation of the time delay τ and embedding dimension are in Figs. 3 and 4.

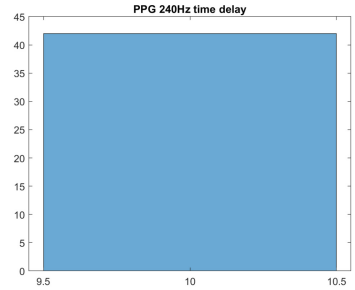

(a) time delay for PPG 240Hz

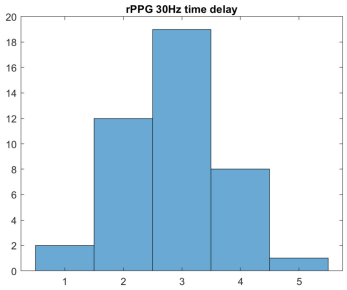

(b) time delay for rPPG 30Hz

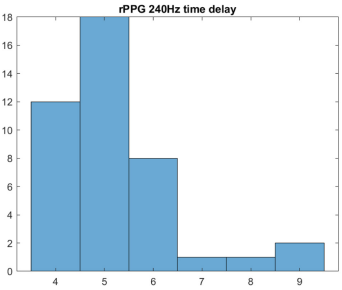

(c) time delay for rPPG 240Hz

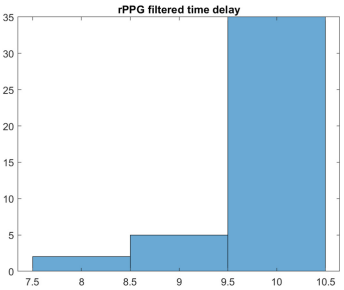

(d) time delay for rPPG filtered

Fig. 3. The estimated time delay τ for 4 signals. Histogram x-axis: the value range of the τ. Histogram y-axis: frequency

The estimated time delay for rPPG 30 Hz is centered and 3. The estimated time delay for PPG 240 Hz and rPPG filtered is mostly at $\tau = 10$ and for rPPG 240 Hz is centered at $\tau = 5$. It shows after the filtering step, the estimated time delay change from 5 to 10. The bandpass filtering for rPPG signal is required to keep the time delay τ similar to the PPG signal after interpolation. The embedding dimension for all signals is either $m = 3$ or $m = 4$. And PPG 240 Hz, rPPG 30 Hz, and rPPG 240 Hz have the majority of the signal from 42 subjects at embedding dimension $m = 4$. After bandpass filtering by continuous wavelet transformation, the rPPG filtered has a majority of embedding dimension $m = 3$. It shows that the postprocessing of the signal by bandpass filtering reduces the complexity of the signal.

An example of the phase space reconstruction result is shown in Fig. 5. The phase space reconstruction result is based on the 4 signals collected and extracted from Subject No. 10. The embedding dimension is $m = 3$ for data visualization purposes. The time delay $\tau = 10$ for PPG 240 Hz and rPPG filtered and $\tau = 3$ for rPPG 30 Hz and $\tau = 5$ for rPPG 240 Hz. The example shows there are similarities between the PPG 240 Hz and the rPPG filtered signal.

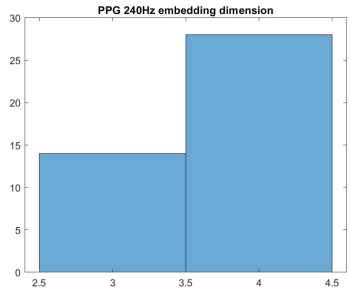

(a) embedding dimension for PPG 240Hz

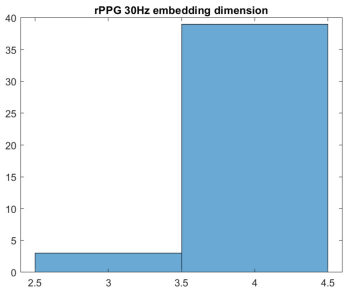

(b) embedding dimension for rPPG 30Hz

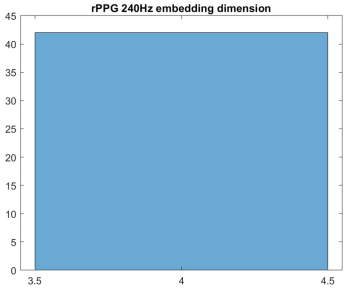

(c) embedding dimension for rPPG 240Hz

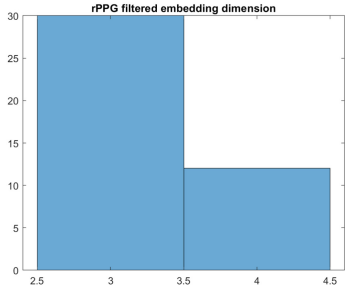

(d) embedding dimension for rPPG filtered

Fig. 4. The estimated embedding dimension m for 4 signals. Histogram x-axis: the value range of the m. Histogram y-axis: frequency

4.3 Lyapunov Exponent

A chaotic system is sensitive to initial conditions. The chaotic level can be quantified by the Lyapunov exponent, which is used to characterize the trajectories in the phase space to measure the rate of divergence of neighboring trajectories. Any chaotic system must have at least one positive Lyapunov exponent. So the largest Lyapunov exponent (LLE) can be used to determine whether a system is chaotic. The algorithm for computing LLE mainly follows [21]. The LLE of all signals is positive, indicating the PPG and rPPG signals are consistent with the definition of a chaos dynamic system.

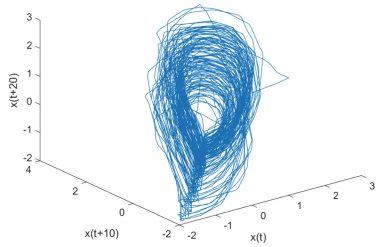

(a) reconstructed trajectories for PPG 240Hz

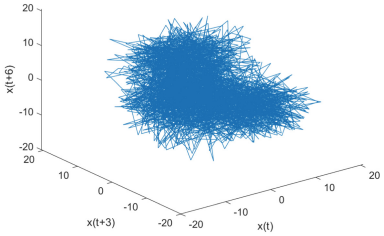

(b) reconstructed trajectories for rPPG 30Hz

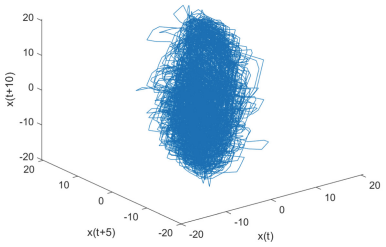

(c) reconstructed trajectories for rPPG 240Hz

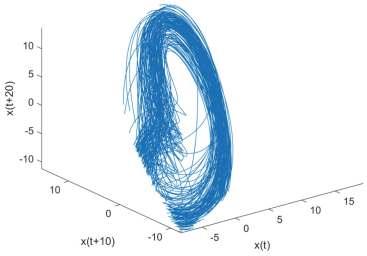

(d) reconstructed trajectories for rPPG filtered

Fig. 5. An example of reconstructed trajectories in $m = 3$ for 4 signals

4.4 Correlation Dimension

The correlation dimension is usually refers to a type of fractal dimension, which measures the dimension of the space occupied by random points. It can be used to separate the chaos from random noise. The correlation dimension is the slope of $C(R)vs.R$, where R is the radius of similarity and $C(R)$ is given by

$$C(R) = \frac{2\sum_{i=1}^{N} N_i(R)}{N(N-1)} \tag{3}$$

where $N_i(R)$ is the number of the points within the range R of point i. The statistical distribution for correlation dimension is in Fig. 6.

The average value for correlation dimension is 2.5022 for ground truth PPG 240 Hz signal. The correlation dimensions are 4.1118 and 3.2700 for rPPG 30 Hz and rPPG 240 Hz respectively. In general rPPG contains more noise from the illumination and the motion of the subject than PPG signals, thus the correlation dimension should be higher. The result rPPG 240 Hz has less correlation dimension than rPPG 30 Hz also indicates the interpolation process reduces the correlation dimension. rPPG filtered has an average correlation dimension value of 2.908, which is less than the unfiltered signal. It means the filtering process

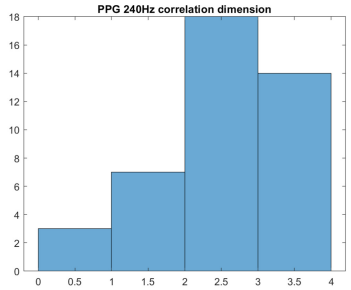

(a) correlation dimension for PPG 240Hz

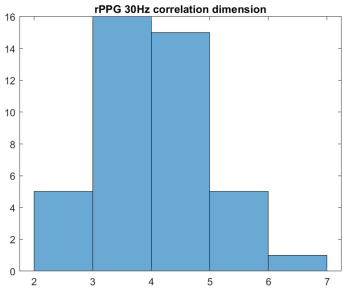

(b) correlation dimension for rPPG 30Hz

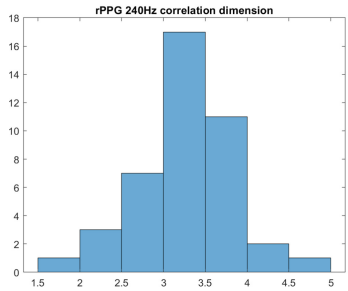

(c) correlation dimension for rPPG 240Hz

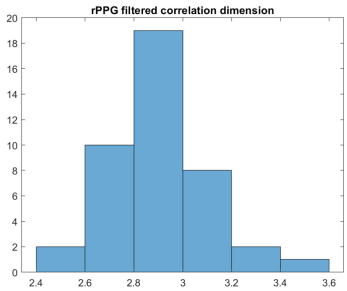

(d) correlation dimension for rPPG filtered

Fig. 6. The estimated correlation dimension for 4 signals. Histogram x-axis: the value range of the correlation dimension. Histogram y-axis: frequency

significant reduces the noise in the rPPG signals. The reduce in the correlation dimension also means the filtered rPPG signal is more close to the ground truth signal.

4.5 Approximate Entropy

The unpredictability of the time series data can be quantified by approximate entropy. A higher value of approximate entropy indicates a higher irregularity and more fluctuations in the uniformly sampled time series data. If more repetitive patterns of a signal is observed, the signal is more predictable and thus has a smaller value of approximate entropy. The complexity level can be quantified by the approximate entropy derived from a time series.

The approximate entropy is calculated as $\phi_m - \phi_{m+1}$, where,

$$\phi_m = \frac{\sum_{i=1}^{N-m+1} log(N_i)}{N - m + 1} \tag{4}$$

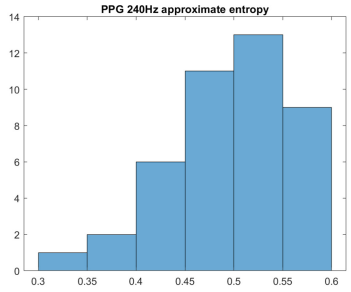

(a) approximate entropy for PPG 240Hz

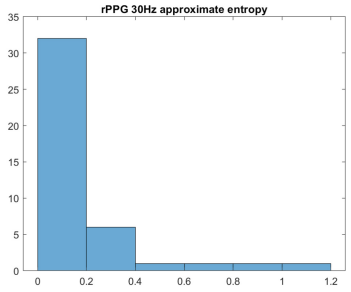

(b) approximate entropy for rPPG 30Hz

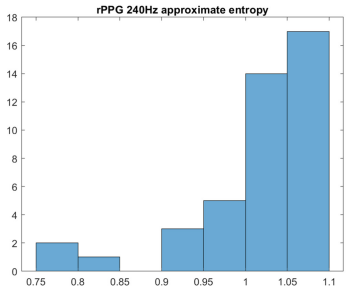

(c) approximate entropy for rPPG 240Hz

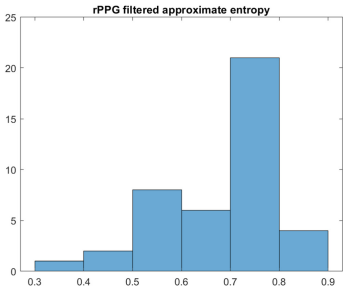

(d) approximate entropy for rPPG filtered

Fig. 7. The estimated approximate entropy for 4 signals. Histogram x-axis: the value range of the approximate entropy. Histogram y-axis: frequency

where m is the embedding dimension, N is the number of data points, N_i is s the number of the points within the radius of similarity R of point i. The statistical distribution for approximate entropy is in Fig. 7.

5 Results

The average value for approximate entropy is 0.4963 for ground truth PPG 240 Hz signal. The approximate entropy are 0.2315 and 1.0156 for rPPG 30 Hz and rPPG 240 Hz respectively. The result rPPG 240 Hz has higher approximate entropy than rPPG 30 Hz indicating the interpolation process increases the approximate entropy and introduces more complexity into the signal. rPPG filtered has an average approximate entropy value of 0.6885, which is less than the unfiltered signal. It means the filtering process will significantly reduce the complexity of the signal. It also means the filtered rPPG signal is more close to the ground truth signal.

The signal properties derived from the reconstructed phase space include Lyanpunov exponent, correlation dimension and approximate entropy. These

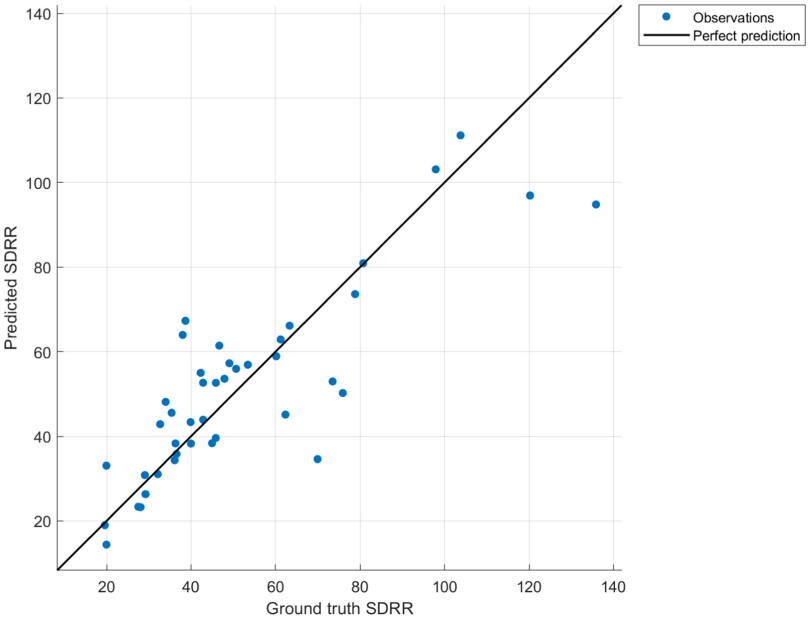

Fig. 8. SDRR results derived from the rPPG filtered (RMSE = 13.72)

properties can be used to improve the current HRV detection method accuracy based on rPPG as an addition feature for a regression model.

After the rPPG signal is derived from the face video (rPPG 30 Hz), interpolated (rPPG 240 Hz), and bandpass filtered (rPPG filtered), the signal is reconstructed by inverse CWT. The peak detection algorithm is used to detect peaks of the signal.

RR interval is defined as the time interval of the consequent peaks.

$$RR_i = PP_i - PP_{i-1} \tag{5}$$

where RR_i is the ith RR interval and PP_i is the time for the ith peak.

We use HRV time domain definitions SDRR. SDRR is defined as standard deviation of all RR intervals, that is

$$SDRR = \sqrt{\frac{\sum_i (RR_i - mean(RR))^2}{N-1}} \tag{6}$$

The HRV result derived from the ground truth signal and rPPG filtered is shown in Fig. 8. With RMSE = 13.72. We can improve the accuracy by building a regression model using 4 features, including the HRV detection results derived from the rPPG, Lyanpunov exponent, correlation dimension and approximate entropy. The HRV result derived from the ground truth PPG240 Hz signal and Gaussian process regression model is shown in Fig. 9 with RMSE = 12.19.

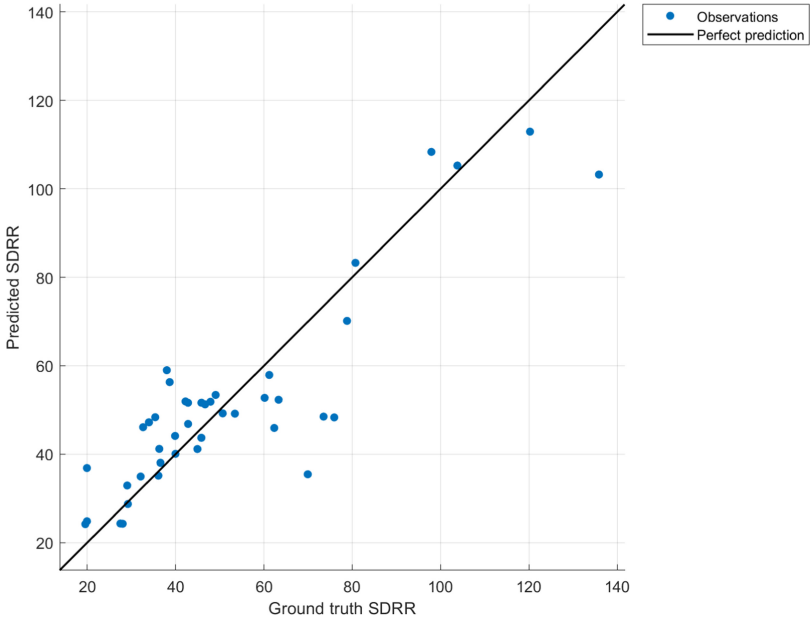

Fig. 9. SDRR results derived from the regression model using HRV detection results derived from the rPPG, Lyanpunov exponent, correlation dimension and approximate entropy (RMSE = 12.19)

6 Conclusion

The main purpose of this study is to investigate rPPG dynamics from nonlinear signal processing techniques. The PPG and rPPG signals obtained from UBFC-rPPG dataset are used for the experiment. The phase space reconstruction methods are applied to test the chaotic characteristics of rPPG dynamics. The obtained results provided strong evidence that rPPG is considered as deterministic chaotic after interpolation and bandpass filtering. Additionally, we discovered the best embedding dimension for the rPPG signal is between 3 to 4. The time delay is 10 for 240 Hz rPPG signal. The phase space reconstruction shows bandpass filtering is required to preserve the topological similarities of the rPPG signal and the PPG signals. The interpolation process will increase the complexity level and reduce the correlation dimension of the rPPG. The bandpass filtering process will reduce the complexity level and the correlation dimension of the rPPG. Including the features such as Lyanpunov exponent, correlation dimension and approximate entropy could reduce the RMSE of HRV detection.

This result provides some insight into the feasibility of using rPPG signal for cardiovascular state monitoring. Nonlinear approaches may become a potential method used to evaluate the quality of different rPPG extraction algorithms. The applications of nonlinear signal methods may also contribute to future studies of human mental and physiological health detection.

Acknowledgement. This project is partially supported by a number of grants from the Ubicomp lab at Marquette University.

References

1. Benjamin, E.J., Muntner, P., Bittencourt, M.S.: Heart disease and stroke statistics-2019 update: a report from the American Heart Association [Internet]. Circulation **139**(10), e56–e528 (2019). https://doi.org/10.1161/CIR.0000000000000659
2. Verkruysse, W., Svaasand, L., Nelson, J.: Remote plethysmographic imaging using ambient light. Opt. Express **16**, 21434–21445 (2008)
3. Sviridova, N., Sakai, K.: Human photoplethysmogram: new insight into chaotic characteristics. Chaos, Solitons Fractals **77**, 53–63 (2015)
4. Charlton, P.H., et al.: Measurement of cardiovascular state using attractor reconstruction analysis. In: 2015 23rd European Signal Processing Conference (EUSIPCO), pp. 444–448. IEEE (2015)
5. Sviridova, N., Zhao, T., Aihara, K., Nakamura, K., Nakano, A.: Photoplethysmogram at green light: where does chaos arise from? Chaos, Solitons Fractals **116**, 157–165 (2018)
6. Sviridova, N., Savchenko, V., Savchenko, M., Aihara, K., Okada, K., Zhao, T.: Reconstructed dynamics of the imaging photoplethysmogram. In: 2018 40th Annual International Conference of the IEEE (2018)
7. Peng, R.-C., Zhou, X.-L., Lin, W.-H., Zhang, Y.-T.: Extraction of heart rate variability from smartphone photoplethysmograms. Comput. Math. Methods Med. **2015**, 516826 (2015)
8. Poh, M.-Z., McDuff, D.J., Picard, R.W.: Non-contact, automated cardiac pulse measurements using video imaging and blind source separation. Opt. Express **18**(10), 10762–10774 (2010)
9. de Haan, G., Jeanne, V.: Robust pulse rate from chrominance-based rPPG. IEEE Trans. Biomed. Eng. **60**(10), 2878–2886 (2013)
10. Huang, R.-Y., Dung, L.-R.: Measurement of heart rate variability using off-the-shelf smart phones. Biomed. Eng. Online **15**(11), 1–16 (2016)
11. Wang, W., den Brinker, A.C., Stuijk, S., de Haan, G.: Algorithmic principles of remote-PPG. IEEE Trans. Biomed. Eng. **PP**(99), 1 (2016). (Posted 13 September 2016, in press)
12. Lewandowska, M., Ruminski, J., Kocejko, T., Nowak, J.: Measuring pulse rate with a webcam - a non-contact method for evaluating cardiac activity. In: Proceedings of Federated Conference on Computer Science and Information Systems, pp. 405–410. IEEE (2011)
13. de Haan, G., van Leest, A.: Improved motion robustness of remote-PPG by using the blood volume pulse signature. Physiol. Meas. **35**(9), 1913–1922 (2014)
14. Wang, W., Stuijk, S., de Haan, G.: A novel algorithm for remote photoplethysmography: spatial subspace rotation. IEEE Trans. Biomed. Eng. **63**(9), 1974–1984 (2016)
15. Unakafov, A.M.: Pulse rate estimation using imaging photoplethysmography: generic framework and comparison of methods on a publicly available dataset. Biomed. Phys. Eng. Express **4**(4), 045001 (2018)
16. Bobbia, S., Macwan, R., Benezeth, Y., Mansouri, A., Dubois, J.: Unsupervised skin tissue segmentation for remote photoplethysmography. Pattern Recogn. Lett. **124**, 82–90 (2017)

17. Viola, P.A., Jones, M.J.: Rapid object detection using a boosted cascade of simple features. In: IEEE CVPR (2001)
18. Lucas, B.D., Kanade, T.: An iterative image registration technique with an application to stereo vision. In: International Joint Conference on Artificial Intelligence (1981)
19. Vezhnevets, V., Sazonov, V., Andreeva, A.: A survey on pixel-based skin color detection techniques. In: Proceedings of Graphicon, vol. 3, pp. 85–92, Moscow (2003)
20. Wang, W., den Brinker, A.C., Stuijk, S., de Haan, G.: Amplitude-selective filtering for remote-PPG. Biomed. Opt. Express **8**, 1965–1980 (2017)
21. Rosenstein, M.T., Collins, J.J., De Luca, C.J.: A practical method for calculating largest Lyapunov exponents from small data sets. Physica D **65**(1–2), 117–134 (1993)